Journal of the Korean Nuclear Society
Volume 36, Number 4, pp.285~294, August, 2004

Pressure Wave Propagation in the Discharge Piping with Water Pool

Young S. Bang, Kwang W. Seul, and In-Goo Kim
Korea Institute of Nuclear Safety
19 Guseong-dong, Yuseong-gu, Daejeon 305-338, Korea
kl64bys@kins.re.kr

(Received January 15, 2004)

Abstract

Pressure wave propagation in the discharge piping with a sparger submerged in a water pool, following the opening of a safety relief valve, is analyzed. To predict the pressure transient behavior, a RELAP5/MOD3 code is used. The applicability of the RELAP5 code and the adequacy of the present modeling scheme are confirmed by simulating the applicable experiment on a water hammer with voiding. As a base case, the modeling scheme was used to calculate the wave propagation inside a vertical pipe with sparger holes and submerged within a water pool. In addition, the effects on wave propagation of geometric factors, such as the loss coefficient, the pipe configuration, and the subdivision of sparger pipe, are investigated. The effects of inflow conditions, such as water slug inflow and the slow opening of a safety relief valve are also examined.

Key Words : pressure wave, propagation, reflection wave, RELAP5/MOD3, water hammer experiment

1. Introduction

An In-containment Refueling Water Storage Tank (IRWST) has been incorporated into the Advanced Power Reactor (APR) 1400 design, as one of the new features designed to enhance safety [1]. One of the important functions of the IRWST is to provide a large water pool to condense steam from the pressurizer during overpressure transients. The Safety Depressurization System (SDS) discharges the high temperature steam from the pressurizer to the IRWST. The major components of SDS are Safety Relief Valves (SRV), piping, and spargers submerged in the pool. Specifically, the SRV has been effectively used to relieve the system pressure following an overpressure transient in nuclear power plants (NPP).

In the course of design, the thermal-hydraulic response of the piping system and the resultant hydrodynamic load on the pipe segments should be evaluated with regard to transients caused by opening the SRV [2]. Such a load is related to the pressure wave propagation along the piping

system, including the submerged pipes, which can be expressed in terms of local density variation with time and pressure gradient over the system. Opening the SRV discharges high temperature steam into the piping system, and it may cause a normal shock in a certain location of the system, due to large pressure difference. It establishes a single-phase, steam-air mixture flow toward the free surface of the water inside the sparger pipe submerged in IRWST. As the pressure wave from the SRV reaches the free surface, a reflection wave toward the upstream will be produced, while a new pressure wave within the water inside the sparger pipe will be generated. The free surface is usually suppressed by the pressure wave and the water level may be lowered. Major concerns in this transient are the possibility of normal shock within the piping, interaction with the moving free water surface, and the formation of a pressure peak inside the submerged pipe. In the safety evaluation of the CE System 80+ [3], particular consideration has been given to the shock and the related hydrodynamic load.

In the SDS of APR-1400 design, the U-shaped pipe (loop seal) at the upstream of the SRV is filled with water to protect the SRV from direct-contacting with the steam of pressurizer. Accordingly, the inflow condition of the SDS piping will be changed from water slug to steam. The duration of the valve opening may also be an important factor on the wave propagation. All the possible cases should be considered in predicting the thermal-hydraulic response [2].

The present study aims to understand the basic thermal-hydraulic behavior, including the pressure wave propagation along the discharge pipe. To achieve this aim, a one-dimensional, two-phase system analysis code, RELAP5/MOD3.3 [4] was used. The code has been verified for this kind of compressible two-phase flow problem and has been known to provide a reasonable prediction [5]. The code has been applied to a KAERI (Korea Atomic Energy Research Institute) small-scale test involving a sparger submerged in a water pool, and the result showed that the code provides a good prediction of pressure response [6]. However, a detailed mechanism of the pressure peak was not sufficiently discussed in terms of wave propagation. In the present study, therefore, a water hammer experiment with voiding [7] is simulated by the RELAP5/MOD3.3 code to confirm its applicability for the prediction of "wave propagation" and the adequacy of the calculation model to be used for an actual SDS piping system. Because the SDS piping of the APR-1400 has quite a complex geometry and the counteractions between the pipe branches increase the difficulty in understanding the overall and local response, a simplification of the geometry to a treatable and understandable level is important. Therefore, a transient analysis was done for a piping system simplified from the actual SDS discharge piping of the APR-1400.

Other objective of this study is to investigate the effects on wave propagation of geometric factors, such as the loss coefficient, the pipe configuration, and the subdivision of the sparger pipe and the effects of inflow conditions, including the duration of valve opening and the loop-seal water slug inflow.

It is believed that the effects of geometric parameters and inflow conditions can be clearly identified, and that understanding of complex behavior in an actual plant can be improved by the present approach.

2. Code Applicability

The RELAP5/MOD3 code [4] has been known to have a general capability to calculate the major two-phase phenomena and non-condensable gas behavior [8]. However, the specific verification of

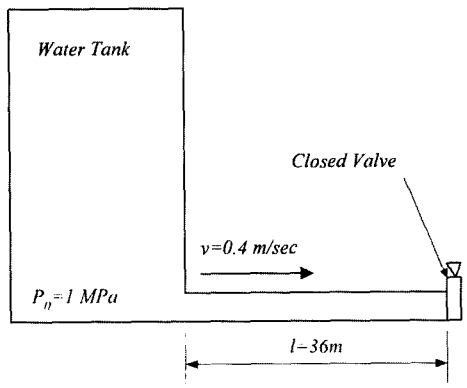

Fig. 1. Schematic Diagram of the Water Hammer Experiment

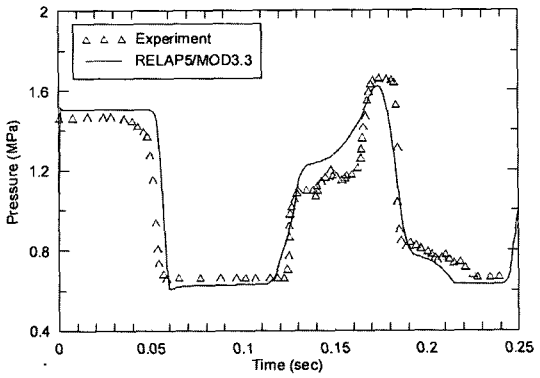

Fig. 2. Comparison of Pressure at the Valve of the Water Hammer Experiment

the code and a modeling scheme suitable to the application are needed to obtain a reliable result, due to the strong dependency on user experience. In this paper, a RELAP5 calculation was performed for a water hammer experiment with voiding [7] to confirm the predictability of the code.

The experiment facility was composed of a large water tank, a horizontal pipe of 36 m, and a quick-closing valve. Initially, the water temperature was 435 K throughout the system and the water was flowing at 0.4 m/sec along the pipe. At time zero, the valve at the end of the pipe was quickly closed, and the pressure at the valve was recorded.

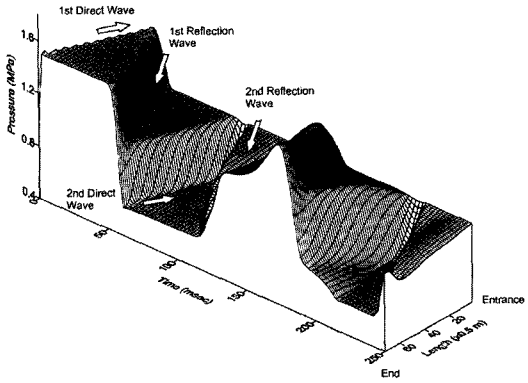

Fig. 3. Pressure Distribution Along the Pipe with Time

During transient, the tank pressure remained at 1 MPa. Figure 1 shows a schematic diagram of the experiment.

For the RELAP5 calculation, a horizontal pipe was modeled with 72 volumes of 0.5 m length and the quick-valve-closing by a trip valve. All the test conditions were modeled as initial and boundary conditions. The valve closure characteristic was not available in the cited reference [7], thus, it was assumed to complete in one time step. The maximum calculation time step was set to 1.0×10^{-4} sec, less than the Courant time limit ($\sim 3.0\times 10^{-4}$ sec), which ensured numerical stability.

Figure 2 shows a comparison of the pressure predicted by RELAP5 with the measured data at the end of the pipe. The RELAP5 pressure response agreed well with the experimental data.

Figure 3 shows the RELAP5-predicted pressure distribution along the pipe over time, which can be interpreted as follows: The pressure at the closed end of the pipe immediately increased when the valve was closed, and the first direct water hammer wave with a positive magnitude of 0.5 MPa was propagated into the upstream. This increased the rear-wave pressure to 1.5 MPa. At about 30 msec, the first direct wave arrived at the pipe entrance, and the first reflection wave was

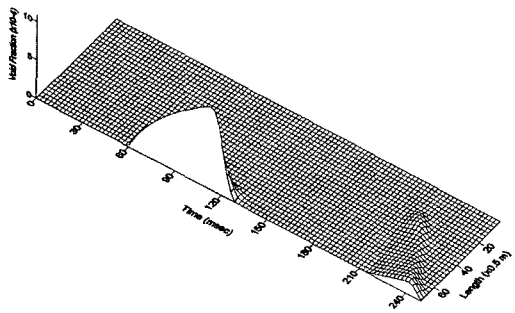

Fig. 4. Void Fraction Distribution Along the Pipe with Time

generated to reserve the inlet boundary condition. The reflection wave was propagated downstream, restoring the rear-wave pressure to 1 MPa. When this first reflection wave reached the pipe end at about 60 msec, the second direct wave was produced by reflection of the reflected wave. It had a negative magnitude to keep the zero velocity at the pipe end. The second direct wave began to move upstream again. At that time, the local pressure dropped to 6.4 MPa, i.e., the saturation pressure corresponding to the local temperature (437 K), which caused flashing at the pipe end (Figure 4). The second direct wave arrived at the pipe entrance in 90 msec, reducing the rear-wave pressure to 0.6 MPa, and the second reflection wave with a positive magnitude was produced and began to travel toward the pipe end. The second reflection wave became weaker as it passed downstream through the pipe, which was obviously due to interaction with vapor bubbles. As a result, the rear-wave pressure was not restored to 1 MPa when the second reflection wave reached the closed end. After the third direct wave began at 120 msec and the void bubbles collapsed, the rear-wave pressure increased to 1.5 MPa, with a delay due to the disappearance of the vapor bubbles. Subsequent behavior was similar to the previous one. Deviation from the previous wave behavior was due to the onset of the two-phase condition and the interaction with vapor

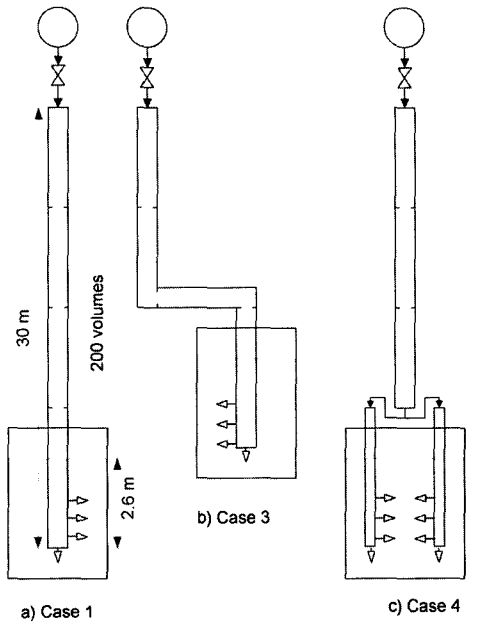

Fig. 5. RELAP5 Models of the Simplified Discharge Piping

bubbles. This indicated that the RELAP5 prediction agreed well with the general theory [9].

A good agreement with the experiment data and with the general theory implies that the code has a general capability to predict wave propagation behavior, although the code has uncertainties, especially in predicting the sound speed and fluid conditions. In addition, it can be concluded that the wave propagation in the actual SDS piping can be predicted with the same degree of accuracy using the RELAP5 code despite the difference in fluid conditions, because it has verified thermal-hydraulic models for a wide range of steam-air mixture conditions.

3. Problem and Modeling

Since the SDS piping network of the APR-1400 has quite a complex geometry and involves a great deal of complicated thermal-hydraulic phenomena, a simplification of the geometric

Table 1. Description of the Calculation Cases

	Symbol ($K_{for/rev}$)	Loss Coef. Geometry	Pipe Pipe	Sparger Condition	Inflow	SRV Opening
Base Case	1	0.0	All Vertical	Single	Steam-air	Quick-open
Geometry Effect	2	1.0 at 3 Junctions	All Vertical	Single	Steam-air	Quick-open
	3	0.0 (0.3/0.3)	Vertical-Horizontal-Vertical	Single	Steam-air	Quick-open
	4	0.0	All Vertical	Double	Steam-air	Quick-open
Inflow Condition Effect	5	0.0	All Vertical	Single	Water Slug ~0.3 sec	Quick-open
	6	0.0	All Vertical	Single	Steam-air (1 sec^{-1})	Linear-open

configuration is needed to understand the wave propagation behavior, as previously discussed. Figure 5 shows a system configuration simplified from the actual SDS discharge piping. It is composed of a source of high temperature steam, an SRV, an SDS pipe, sparger holes, and a water pool. As shown in Figure 5, a single vertical pipe 30 m (100 ft) in length was considered. It was nearly the same height as in an actual plant. The area of the pipe was assumed to be 0.01856 m^2 (0.2 ft^2), and the remaining parameters were appropriately scaled down from the APR-1400.

The pipe was modeled with 200 volumes. At the submerged section of the pipe, four junctions were provided to model the sparger holes. Each junction was connected to the water volume with a hydrostatic pressure that corresponded to its elevation. The default choking model of the RELAP5/MOD3.3 code was applied to all the internal junctions. As an initial condition, steam-air mixture at atmospheric pressure and 322 K (120°F) for the pipe, subcooled water at 322K for the water pool, and saturated steam at 18.7 MPa for the source were assumed, respectively. The initial submerged level was about 2.6 m (7.8 ft) from the bottom of the sparger pipe. As a boundary condition, the SRV was assumed to open instantaneously at time zero, and the water pool pressure remain constant. The maximum time step was 1.0×10^{-4} second, as used in Section 2. This time step size was also verified by the preliminary analysis [10].

In the base case, instantaneous opening of SRV and discharge into vertical pipe was assumed. In addition, the effects of geometric factors, such as loss coefficient at the junction of pipe, inclusion of horizontal pipe segment, and use of two sparger pipes, were investigated. Effects of inflow conditions were also examined, for the case of inflow of a highly subcooled water slug and the case of a slow valve opening, respectively. Table 1 summarizes the calculation cases.

4. Results and Discussion

4.1. Basic Behavior

Figure 6 shows the pressure distribution along the pipe over time for Case 1. As the SRV opened, the pressure at some nodes of the SRV

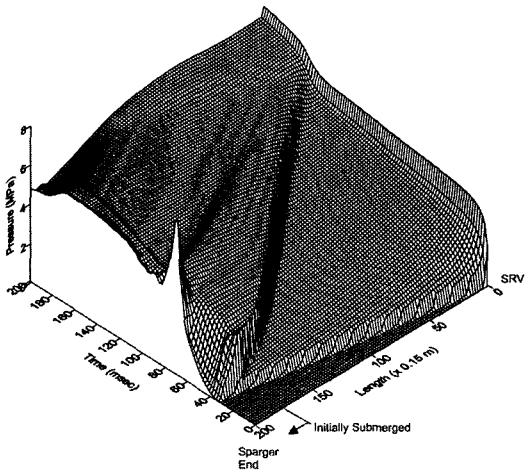

Fig. 6. Pressure Distribution Along the Pipe with Time of the Base Case

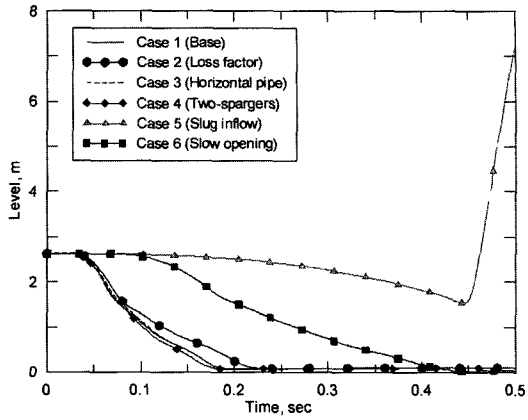

Fig. 7. Comparison of Water Level of the Sparger Pipe

downstream continued to increase over time, while the remaining nodes were unchanged for a short time. This implies a pressure wave propagating into the downstream of the pipe with a steep pressure gradient. This pressure gradient within one or two nodes can be regarded as a normal shock, although the magnitude was not significant and a sharp shock front was not detected, due to the numerical diffusion of the calculation.

As the pressure wave reached the water surface at about 35 msec, a reflection wave was generated from the free surface and began to travel upstream with the same speed as the previous pressure wave. This reflection wave induced a new pressure wave into the submerged portion of the pipe, which resulted in a sudden pressure increase to 3.5 MPa, at 35 msec. The level of water surface began to decrease from 50 msec (Figure 7). It played a part in reducing the speed of the reflecting wave traveling upstream. The reduction of wave speed and the continuous increase of upstream pressure resulted in a weak gradient of the reflection wave. As a result, no significant gradient was found in the subsequent behavior for up to 300 msec.

In the water-submerged field, a peak pressure with a magnitude of 8 MPa occurred at 70 msec, caused by the new pressure wave, the water level suppression, and the interaction of the two.

4.2. Effects of Geometry

Usually in a 1-D approach like RELAP5, a loss coefficient has been used in modeling the actual piping configuration, including bend, tee, elbow, reducer, orifice, etc., and this may have an effect on the wave behavior different from the case that does not include a loss coefficient. Thus, the effect of a loss coefficient was evaluated in Case 2. A loss coefficient was imposed to the internal three junctions and the value of the loss coefficient was arbitrarily selected (K=1.0). In addition, since a horizontal pipe was not considered in Case 1, the effect of the inclusion of the horizontal segment among the vertical pipe was investigated in Cas 3. The loss coefficients K at the elbows was set to 0.3. The SDS piping of the APR-1400 design has several sparger pipes, necessitating an examination of the effects of division of single pipe into several sparger pipes. Thus, the effects of sparger pipe division were evaluated in Case 4.

4.2.1. Effect of Loss Factor

Figure 8 shows a pressure distribution along the pipe over time for Case 2. It can be seen that the basic propagation behavior was similar to the Case 1, although pressure jumps occurred at each junction where the loss coefficient was imposed. It was also found that the reflection wave was propagated from those junctions in the upstream direction. In the meanwhile, the reflection wave generated from the downstream water surface also reached those junctions with a loss coefficient. As a result, the overall pressure distribution became flatter than that of the case without a loss coefficient. In addition, the pressure peak in the submerged section was lower than that of the case without a loss coefficient, which seemed to be due to the loss of wave energy.

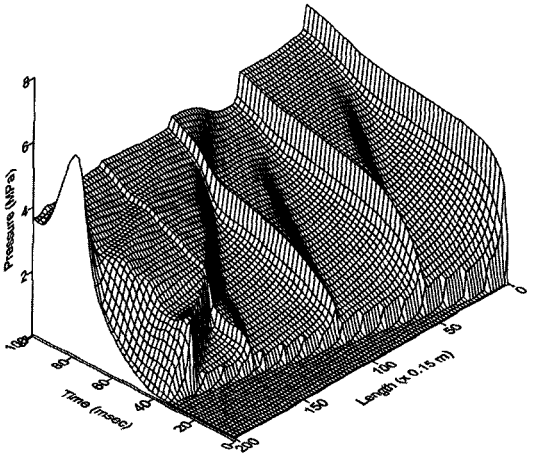

Fig. 8. Pressure Distribution Along the Pipe with Time for the Case with Loss Coefficient

4.2.2. Effect of Horizontal Piping

Figure 9 shows the pressure distribution for Case 3 (horizontal piping). The overall behavior was very similar to that of Case 1, while the waves generated at the junctions with loss showed similar

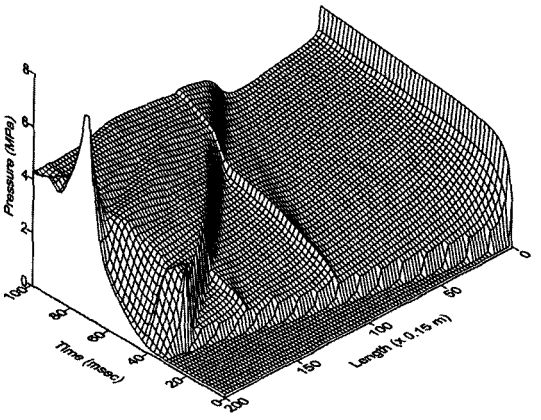

Fig. 9. Pressure Distribution Along the Pipe with Time for the Case with Horizontal Pipe

behavior to those of Case 2. The magnitude of the pressure peak of the submerged section is also similar to that of Case 1. It is obvious that the basic pressure propagation is not changed by the pipe angle and that only the effect of the loss factor can be observed, as in Case 2.

4.2.3. Effect of Division of Sparger

Figure 10 shows the pressure distribution for Case 4 (two-spargers). The overall behavior was similar to that of Case 1. This indicated that the

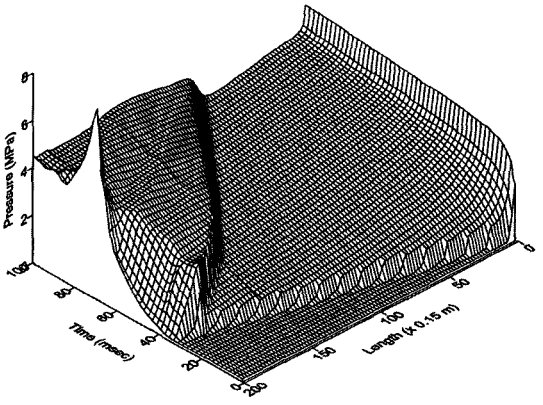

Fig. 10. Pressure Distribution Along the Pipe with Time for the Case with Double Sparger Pipe

division of single sparger pipe into two pipes did not have any influence on the pressure wave propagation and peak pressure at the submerged section, since the physical parameters were the same, including the total volume and the inlet/outlet flow area. A slight deviation from Case 1 was due to the loss factor at the dividing junction, which was automatically set by the code.

4.3. Effect of Inflow Conditions

In the APR-1400 design, a water slug will travel into the SDS piping via an opening in the SRV. A few seconds will pass, from the time of the SRV actuation signal to the time at which the valve is fully open. Accordingly, the water slug inflow and the slow valve opening may cause different effects from those of the base case. The following sections examine such effects.

4.3.1. Effect of Water Slug Inflow

In this analysis, highly-subcooled water of (120°F) was assumed to maximize the water slug size conservatively. In addition, the water was assumed to move into the SDS piping for 0.3 sec after opening the SRV, based on the APR-1400 design.

Figure 11 shows a pressure distribution along the pipe for Case 5 (water slug inflow) up to 100 msec. The magnitude of the wave was very small and the speed of the wave propagation and reflection was slower than in Case 1. Thus, one can conclude that a significant pressure gradient would not be expected in the early transient. Figure 12 shows a pressure distribution from 300 to 500 msec, which corresponded to the period of the water slug traveling through the pipe. A pressure wave with a magnitude greater than 8 MPa traveled downstream. The magnitude gradually increased, while the wave front became

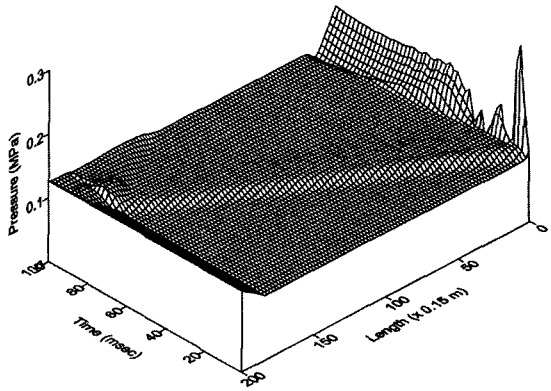

Fig. 11. Pressure Distribution Along the Pipe with Time for the Case with Water Slug Inflow (before water slug entrance)

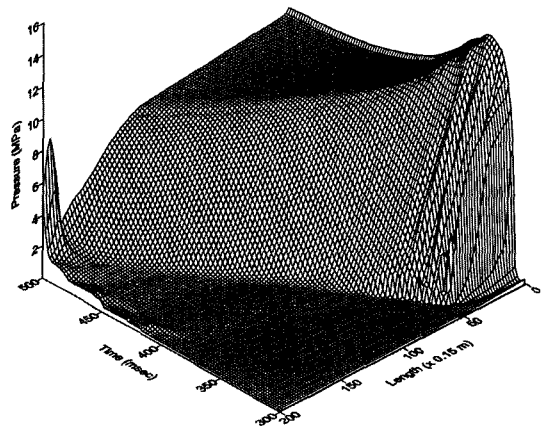

Fig. 12. Pressure Distribution Along the Pipe with Time for the Case with Water Slug Inflow (after water slug entrance)

smoother over time; therefore, a significant pressure gradient was not expected. However, in the submerged section, the peak pressure rose to 8 MPa, as the pressure wave front reached the free surface, and this may significantly contribute to the hydrodynamic load. Figure 13 shows the water slug movement behavior in this case, which showed that the water slug moved downstream, increasing the rear-side steam pressure to more than 10 MPa. The pressure of the submerged section increased immediately when the density

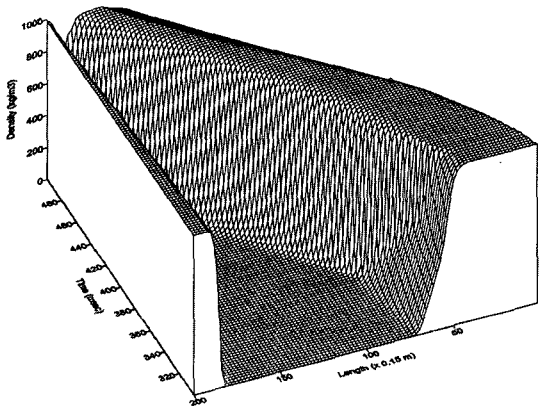

Fig. 13. Density Distribution Along the Pipe with Time for the Case with Water slug Inflow (after water slug entrance)

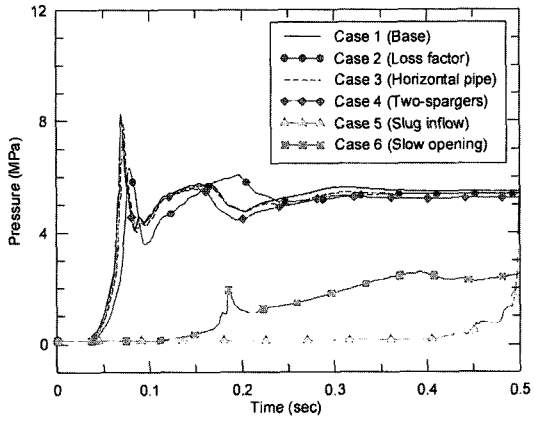

Fig. 15. Comparison of Pressure at the Sparger Pipe End

wave reached the free surface. Thus, it should be emphasized that the water slug inflow has the effect of minimizing the pressure peak in the very early period; however, it may cause an immediate pressure peak in the submerged section in later phase.

4.3.2. Effect of Valve Opening Time

Figure 14 shows a pressure distribution for Case 6 (linear SRV opening during 1 second). Compared to Case 1, very weak and slow pressure wave propagation was observed. This was clearly due to the slow increase of the inlet flow. The reflection wave from the water surface was found at about 60~70 msec seconds, and the submerged water level started to decrease from 0.1 seconds, as shown in Fig 6. As a result, the pressure peak in the submerged section was about 2 MPa at 0.2 second. This prediction implied that a gradual opening of the SRV could reduce the immediate peak pressure.

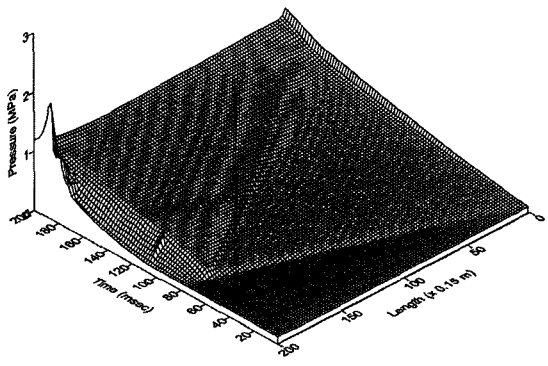

Fig. 14. Pressure Distribution Along the Pipe with Time for the Case with Linear SRV Opening

Figure 15 shows a comparison of the pressure at the end of the sparger pipe for the cases discussed above. The peak pressure was found to be 8 MPa for the SRV quick-opening cases while and 3 MPa for the SRV slow-opening-case.

5. Conclusions

To understand the thermal-hydraulic response of a safety relief valve discharge pipe of with water pool, a simplified problem was analyzed using a one-dimensional, two-phase flow analysis code, RELAP5/MOD3.3. The applicability of the code was assessed for an experiment involving a water hammer with voiding. The experimental result

supported the applicability of the code and the adequacy of the present modeling. The pressure wave propagation behavior was investigated, and the effects of geometric factors and inflow conditions were examined. From the present study, the following conclusions were obtained:

1) The RELAP5/MOD3.3 code and the present modeling scheme can be applied to a wave propagation analysis, such as one involving a water hammer with voiding.
2) The basic thermal-hydraulic response can be expressed in terms of the pressure wave propagation, the reflection wave from the free water surface, and the interaction of the two. The pressure peak and steep gradient were observed in the submerged section of the pipe, as a result of the interaction between the wave and the moving free surface
3) The loss factor has the effect of inducing a slight pressure jump at the junction and generating a reflection wave into the upstream. A slug inflow has the effect of suppressing the initial pressure peak. A gradual opening of the safety relief valve can significantly reduce the magnitude of the pressure wave and the immediate peak pressure that occurs when the water slug meets the free surface.

Future research will involve an analysis of an actual safety depressurization system using the analysis scheme presented in this paper.

References

1. Korea Electric Power Corp., *Korean Next Generation Reactor Standard Safety Analysis Report*, Seoul (1998).
2. United States Nuclear Regulatory Commission, *Standard Review Plan*, USNRC, Washington, D.C., NUREG-0800. (1988).
3. United States Nuclear Regulatory Commission, *Final Safety Evaluation Report Related to the Certification of the System 80+ Design*, USNRC, Washington, D.C., NUREG-1462, August (1994).
4. Information System Laboratory Inc., RELAP5/MOD3.3 Code Manual, Rockville, MD, NUREG/CR-5535 (2002).
5. Stubbe, E.J., Vanhoenacker L., and Otero, R., *RELAP5/MOD3 Assessment for Calculation of Safety and Relief Valve Discharge Piping Hydrodynamic Loads*, USNRC, NUREG/IA-0094 (1990).
6. G.B.Doh, et al., Evaluation of the Reflooding Behavior of Blowdown and Condensation (B&C) Loop with a Prototype Sparer Using the RELAP5 Code, Paper 3345, Proceedings of ICAPP' 03, Cordoba, Spain, May (2003).
7. B.Mavko, et al., *A Sketch of a Facility for Water Hammer Problem, CAMP Activity in Slovenia*, Presented at the CAMP Meeting, Washington D.C., October (1996).
8. Kwang W. Seul, et al., Simulation of Multiple Steam Generator Tube Rupture (SGTR) Event Scenario, Journal of KNS, Vol. 35, No. 3, pp 179~190, June (2003).
9. G.V.Aronovich, et al., Water Hammer and Surge Tanks, Izdatel' stvo "Nauka", Moskva (1968).
10. Young S. Bang, et al., Thermal-hydraulic Response in the Discharge Piping with Water Pool, PVP-Vol.435, 2002 ASME Pressure Vessels and Piping Conference, Vancouver, Canada, August (2002).